Local disorder in crystalline and amorphous germanium

G. Dalba, P. Fornasini, and M. Grazioli
Dipartimento di Fisica dell'Università degli Studi di Trento, I-38050 Povo, Trento, Italy

F. Rocca
Centro di Fisica degli stati aggregati ed impianto ionico del Consiglio Nazionale delle Ricerche, I-38050 Povo, Trento, Italy
(Received 19 May 1994; revised manuscript received 23 November 1994)

Anharmonic contributions to the pair potential of near-neighbor interactions of crystalline and amorphous germanium have been determined by temperature-dependent x-ray absorption fine structure measurements. The measurements have been carried out at the K edge of Ge in the temperature range 77–450 K and analyzed by the cumulant method. In c-Ge the temperature dependence of the first four cumulants has been determined for the first three coordination shells. The radial distribution function of the nearest-neighbor atoms has been found Gaussian in the examined temperature range; the second and third shell distance distributions show a symmetric but non-Gaussian behavior even below the Debye temperature. Cumulants have been related to the force constants of the effective pair potential. The harmonic contribution to thermal disorder has been extracted from the second cumulant for each coordination shell and compared with the mean square relative displacements calculated by harmonic models of lattice dynamics; experimental results are in good agreement with theoretical calculations. In amorphous germanium the first shell radial distribution function is asymmetric even at the lowest temperatures. Static and dynamic effects to the local disorder have been separately determined and compared with the results of previous studies.

I. INTRODUCTION

Extended x-ray absorption fine structure (EXAFS) is recognized as a particularly useful tool for studying the local structure of disordered materials. It provides information about near-neighbor distances, coordination numbers, and disorder in bond distances. Moreover, temperature-dependent measurements of the amplitude and phase of EXAFS oscillations allow one to separate thermal from static disorder and to characterize anharmonic pair potentials and asymmetric pair distribution functions.[1] One of the ways to investigate local disorder by EXAFS is the cumulant method. This model-independent technique is based on the expansion of EXAFS amplitudes and phases as a series of cumulants of the interatomic distance distribution.[1] The first cumulant is related to the centroid of the distribution, the second one is the variance and corresponds to the mean square relative displacement (MSRD) σ^2, and higher order cumulants characterize the deviation of the distribution of distances from a harmonic Gaussian shape. The cumulant method is appropriate for systems characterized by low or moderate anharmonic disorder.

Remarkable EXAFS works on crystalline and amorphous germanium are present in the literature.[1,2] In most of them the local structure in c-Ge and a-Ge has been studied by standard EXAFS analysis. The standard analysis is based on the harmonic approximation and accounts for local disorder by the EXAFS Debye-Waller factor $\exp(-2k^2\sigma^2)$. Some works are concerned with the temperature dependence of σ^2 and its interpretation in terms of simple models of vibrational dynamics. Stern *et al.*[3] studied the thermal variation of disorder about the first and second average shell distances in c-Ge and found that first shell $\sigma^2(T)$ was adequately represented by an Einstein model and the second shell $\sigma^2(T)$ was fitted by a Debye model.

Tests for detecting the asymmetry in the distributions of atoms in Ge were examined by Crozier and Seary[4] who carried out EXAFS measurements in the range $T = 83$–1085 K. They found that in a-Ge the distribution of nearest neighbors is Gaussian while in c-Ge it presents a small asymmetry at the highest temperatures. Other significant EXAFS works on Ge are concerned with the structural relationship between c-Ge and a-Ge and the transition from amorphous to crystalline phase;[5,6] thin films of Ge were prepared according to different techniques at different substrate temperatures.[6,7] A methodical characterization of vacuum deposited amorphous Ge was carried out by Johnson *et al.*[8] who investigated crystallinity in amorphous films by analyzing the Fourier transforms of the second and third neighbors.

The aim of this work is to study the local structure and dynamics of c-Ge and a-Ge beyond the harmonic approximation by exploiting the sensitivity of EXAFS spectroscopy to anharmonic effects. We present the temperature dependence of the first four cumulants of the radial distribution functions relative to the first three coordination shells of c-Ge. By determining the force constants of the EXAFS pair potentials of near-neighbor interactions we evaluate the harmonic contribution to the MSRD and compare it with refined models of vibrational dynamics. As for a-Ge, we are able to reconstruct the first shell distance distribution from the first four experi-

mental cumulants and to separate the thermal and static contributions to disorder.

The paper is organized as follows. In Sec. II a summary of the cumulant method is presented. Sections III and IV describe experimental details concerning sample preparation, measurements, and data analysis. Sections V and VI are devoted to the presentation and discussion of results; the summary and conclusions are given in Sec VII.

II. ANALYTICAL METHOD

Single shell structural parameters were determined by applying the cumulant expansion method:[1] this nonstandard EXAFS analysis is useful for moderately disordered systems where the radial distribution is insufficiently approximated by a Gaussian. The need for an EXAFS theory which took into account systems with non-Gaussian pair distribution functions was pointed out by Eisenberger and Brown.[9] The capability of EXAFS to determine the details of the nearest-neighbor pair distribution and to study the anharmonic short range pair interaction potentials was demonstrated by Hayes and Boyce.[10] The expansion of asymmetric pair correlation functions in terms of cumulants in EXAFS was suggested by Rehr (see Ref. 11); a detailed description of the cumulant method was given by Bunker;[12] the sensitivity of EXAFS to anharmonic effects and its capability to give unique information about anharmonic interactions was exploited by Tranquada and Ingalls.[13] Finally, the topic has been reviewed by Crozier *et al.*[1] and is currently applied to investigate the structure and dynamics of disordered systems.[14–16] In terms of the cumulants C_i the EXAFS function is expressed as

$$\chi(k) = A(k)\sin[\Phi(k)]$$

with amplitude $A(k)$ and phase $\Phi(k)$ given by

$$A(k) = \frac{S_0^2}{kR^2} NF(k)\exp\left(C_0 - 2C_2k^2 + \frac{2}{3}C_4k^4 + \cdots\right), \tag{1}$$

$$\Phi(k) = 2kC_1 - \frac{4}{3}C_3k^3 \cdots + \phi(k),$$

where S_0^2 takes into account the intrinsic inelastic effects, k is the photoelectron wave vector, N the coordination number of the specific shell, $F(k)$ the backscattering amplitude, and $\phi(k)$ the total phase shift between absorbing and backscattering atoms. For narrow distributions $\exp(C_0) \approx \exp(-2C_1/\lambda)/C_1^2$,[16] where λ is the photoelectron mean free path. Even and odd cumulants can be extracted from Eqs. (1) by resorting to a standard compound or to theoretical calculations which provide the parameters S_0^2, $F(k)$, and $\phi(k)$. In the present analysis we have referred to internal standards: crystalline and amorphous germanium at the lowest measured temperature, i.e., 77 K.

III. EXPERIMENTAL DETAILS

The c-Ge samples were prepared by powdering a high purity Ge monocrystal; the powders were deposited, by the sonication method, on polytetrafluoroethylene filters in order to get homogeneous samples of uniform thickness, as required by x-ray absorption measurements in transmission mode. The a-Ge samples were prepared by thermal evaporation of pure monocrystalline Ge onto a thin Al foil at 10^{-6} Torr; the temperature of the substrate was $160 \pm 10\,^{\circ}\mathrm{C}$ and the deposition rate 5 μm/h. The amorphicity of the sample was checked by x-ray diffraction measurements. The average dimensions of the powder grains and thickness of crystalline and amorphous samples were chosen in such a way as to avoid thickness effects[17] and to maximize the signal to noise ratio. The absorption edge jump at the K edge of Ge was $\Delta\mu x = 1$, where μ is the absorption coefficient and x the sample thickness. Independent sets of EXAFS measurements at the K edge of c-Ge were performed at both the beamlines BX1 and BX2-S of the storage ring Adone at the PWA laboratory in Frascati. The electron beam energy was 1.5 GeV and the maximum injected current 60 mA. The monochromator was a channel-cut silicon crystal with reflecting faces (111) at BX1 and Si (220) at BX2-S. The a-Ge sample was investigated at the BX2-S beamline in Frascati and at the EXAFS-3 beamline of the storage ring DCI at LURE laboratories in Orsay. The beam energy of DCI was 1.85 GeV and the injected current $\approx$ 300 mA; the monochromator consisted of two parallel flat Si (311) crystals which could be slightly detuned relative to each other to minimize the harmonic content of the x-ray beam. Absorption spectra were recorded by two ionization chambers filled with krypton at the PWA facilities, and with air at the LURE beamline. The temperature was changed between 77 and 450 K in nine steps by temperature controlled nitrogen flow cryostats and electrical heaters; the sample temperature uncertainty was estimated to be less than 2 K. The availability of several measurements carried out on different experimental apparatuses allowed a more accurate evaluation of the overall uncertainty.

IV. DATA ANALYSIS

The EXAFS signal was extracted from the experimental spectrum in the conventional way[16] assuming the photoelectron binding energy E_0 at the maximum of the first derivative of the spectrum. The $k\chi(k)$ signals of c-Ge and a-Ge are shown in Fig. 1 for some temperatures: thermal damping is evident for both samples. The spectra of a-Ge [Fig. 1(b)] are less structured than the c-Ge ones [Fig. 1(a)] indicating that, due to static disorder, the EXAFS of a-Ge comes from the contribution of only one coordination shell, unlike c-Ge where $k\chi(k)$ is the summation of the contributions of several shells. This situation is clearly depicted in Fig. 2 where the Fourier transforms of $k^3\chi(k)$ are shown. In Fig. 2(a) three prominent peaks, corresponding to the first three coordination shells, are evident; in Fig. 2(b) only one peak is present confirming that only the first coordination shell contributes to

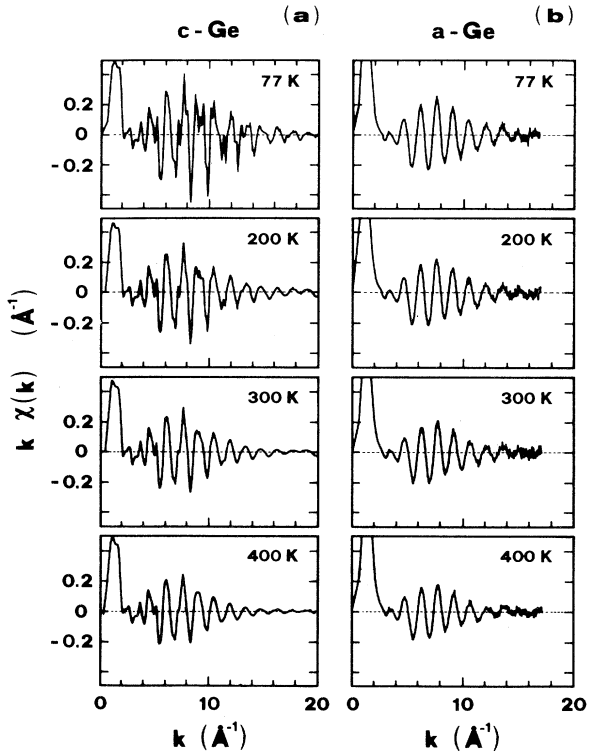

FIG. 1. $k\chi(k)$ XAFS signals at the K edge of Ge of crystalline (a) and amorphous Ge (b) at various temperatures.

the EXAFS signal whereas outer shells are not observed because of thermal and static disorder and lack of low k information.[18] EXAFS contributions of the first three coordination shells of c-Ge and the first shell of a-Ge were singled out by back-transforming each peak in Fig. 2 to k space (the r-space back-transforming intervals are indicated by horizontal segments in Fig. 2). The Fourier filtering procedure allows one to separate the EXAFS

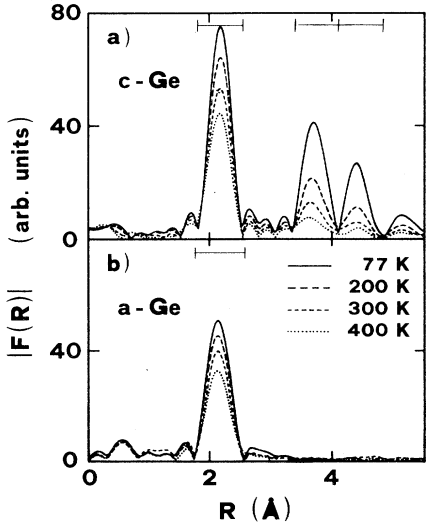

FIG. 2. Fourier transforms of the XAFS signals shown in Fig. 1 for c-Ge (a) and a-Ge (b). A k^3 weighting factor and a 10% Hanning window have been used for both c-Ge and a-Ge.

amplitudes $A(k)$ and phases $\Phi(k)$ of each coordination shell. The peaks relative to the first three shells of c-Ge [Fig. 2(a)] are well defined and separated; however, the second and third peaks are very close to each other. In this case a mutual interference of the two peaks is expected; it could reduce the accuracy of the structural parameters obtained through a separate analysis of the corresponding coordination shells. A simulation test, which will be described in Sec. V when discussing the overall accuracy of results, has allowed us to verify that the errors induced by the interference between the second and third shell peaks in Fig. 2(a) are of the same order of magnitude as the statistical errors of the data analysis, and in any case do not affect in a sensible way the main conclusions of this work. As a consequence we back transformed the three main peaks of Fig. 2(a) and separately analyzed the EXAFS amplitudes $A(k)$ and phases $\Phi(k)$ of each coordination shell by the ratio method. In this way experimental values of backscattering amplitudes, phase shifts, and inelastic terms were taken, separately for each coordination shell, from the low temperature reference spectrum, and the correlation between parameters was reduced to the one between pairs of cumulants. The alternative procedure of a nonlinear fit to the overall contribution to EXAFS of the second and third shells was considered less reliable, in view of (a) the correlation between a large number of parameters to be simultaneously determined, and (b) the need to use backscattering amplitudes, phase shifts, and anelastic terms calculated or extracted from the experimental EXAFS of a different shell (the first one).[1]

The presence of multiple scattering contributions could, however, reduce the accuracy of structural parameters obtained by amplitude and phase analysis. Multiple scattering effects are absent in the first shell and were considered negligible in the second one by Stern *et al.*[3] This result seems to be typical for crystalline compounds with *open* structures like the diamond or zinc-blende structure [for instance, GaAs (Ref. 19)]. Anyway we checked the influence of multiple scattering on the first three coordination shells of c-Ge by *ab initio* calculations on a cluster of five coordination shells of Ge atoms, using the FEFF code.[20] We found that no multiple scattering effects are present in the first shell, they are also negligible in the second one, and a small contribution due to double and triple scattering, which is less than 10% of the single scattering, influences the third coordination shell.

The relative values of the first four cumulants, $\Delta C_i = C_i(T) - C_i(77)$, i =1–4, have been determined for each coordination shell by means of the amplitude ratio and phase difference methods.[16] The cumulant series has been truncated at the fourth-order term: some tests on model distributions representing systems affected by disorder larger than or comparable to that of germanium have shown that the first four cumulants are enough to adequately reproduce the original distributions.[16] The four polynomial coefficients obtained by the fitting procedure constitute a good approximation to the exact cumulants of the *effective* distance distribution only when the cumulant series is rapidly convergent.[16] The validity of this

working assumption for Ge has been checked by verifying that the values of cumulants were independent of the chosen k fitting interval.

A. Crystalline germanium

In Fig. 3 we report the logarithm of the amplitude ratios (solid lines) and the phase differences for the first shell of c-Ge together with the relative best fitting polynomials (dotted lines); the fit was done in the k range 3–18 Å^{-1}. The analogous curves for second and third shells deviate from linearity with increasing temperature; this fact is indicative of non-Gaussian distance distributions in the outer shells as has been already observed in GaAs.[21] Shorter k intervals were used for second and third shells because of lower signal to noise ratios. In all three cases the ratio N_s/N_r was fixed to 1.

B. Amorphous germanium

The logarithm of amplitude ratios and phases differences, using 77 K c-Ge as reference, are reported in Fig. 4; a pronounced deviation from linearity is evident even at low temperature. The fitting procedure of the amplitude ratio has been done either setting the ratio N_s/N_r equal to 1 or leaving it as a free parameter.

V. RESULTS

A. Crystalline germanium

In Fig. 5 the values of the cumulants of the effective distribution for the first three coordination shells of c-Ge are shown vs temperature. From ΔC_1 one can obtain ΔR [Eq. (7) in Ref. 16] by assuming that the radial distribution of distances at 77 K is a narrow Gaussian centered at the crystallographic distance. For the second cumulant the absolute value has been obtained by shifting the experimental ΔC_2 data to match the slope of the Einstein model which best fits the experimental data at high temperature.[1] The difference of MSRD between effective and real distributions will be discussed below. We have assumed $\Delta C_3 = C_3$ and $\Delta C_4 = C_4$. The theoretical curves AT^3 best fitting the fourth cumulants of the second and third shells are also reported in the same figure; the coefficients A are shown in Table I. The standard deviation for each experimental point in Fig. 5 has been calculated by the error analysis carried out on the results obtained from different measurements at the same temperature and by varying the characteristic parameters of the EXAFS data reduction procedure. As was pointed out in Sec. IV, a possible cause of inaccuracy is the mutual interference of second and third shell peaks. To evaluate the influence of this effect on the final results, we used the following test procedure. Two pairs of distributions of distances were calculated starting from the experimental cumulants of second and third shells (Fig. 5) at different temperatures; three different EXAFS functions were simulated and Fourier transformed for each temperature: two based on the two separate distributions (case 1) and one based on the sum of the two distributions (case 2); case 2 corresponds to the experimental situation of Fig. 2(a), in which the mutual influence of the two peaks cannot be disentangled. In both cases 1 and 2 the peaks were isolated, back transformed, and analyzed at the various temperatures by the ratio method. The difference between the cumulants obtained in case 1 and case 2 is comparable with the error bars appearing in Fig. 5, in the whole temperature range. In particular, for the second cumulant the difference at 300 K amounts to 0.8% and 2.4% for the second and third shell, respectively.

From a comparative analysis of the cumulants of the first three shells (Fig. 5) we deduce the following. (a) ΔC_1 as well as ΔR [which is reported in Fig. 6 (crosses)] are close to zero for all shells; experimental uncertainty is larger than the thermal expansion effect in the examined temperature range. (b) The second cumulant, at a given

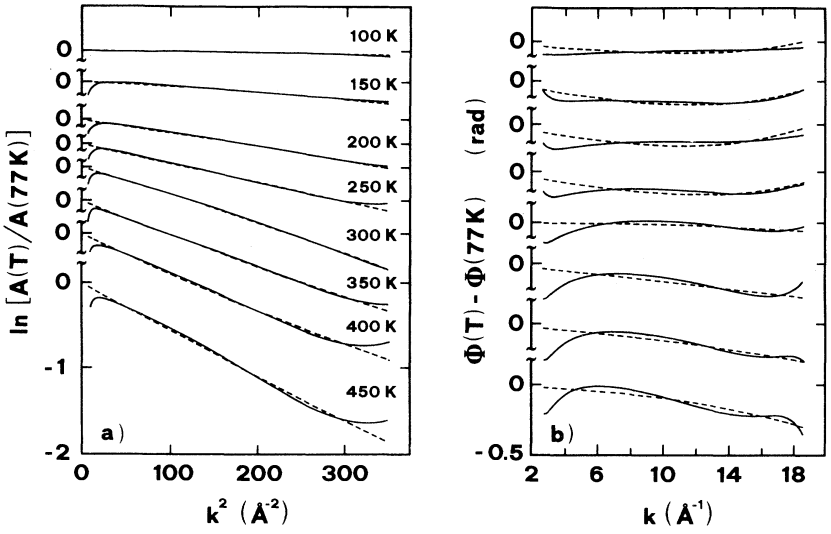

FIG. 3. First coordination shell of c-Ge: (a) logarithm of amplitude ratios vs k^2; (b) phase differences vs k (full lines) and relative best fitting polynomial curves (dashed lines).

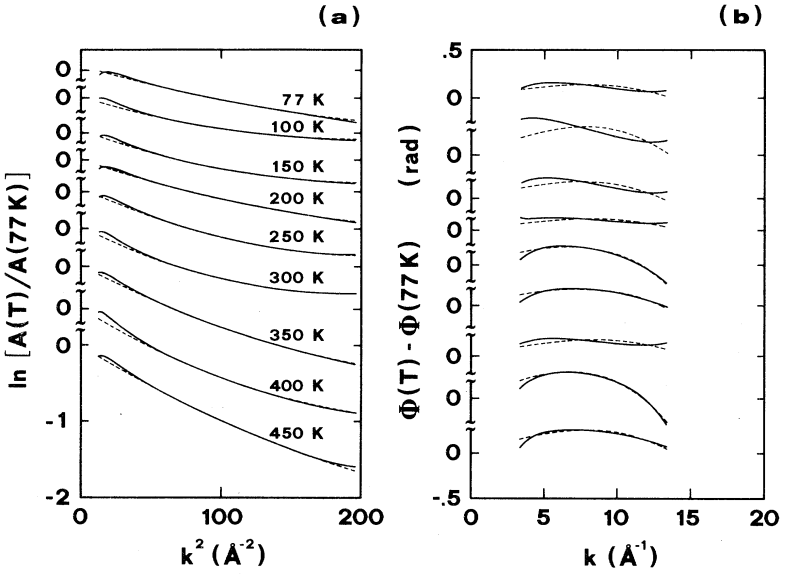

FIG. 4. First coordination shell of a-Ge: (a) logarithm of amplitude ratios vs k^2; (b) phase differences vs k (full lines) and relative best fitting polynomial curves (dashed lines). Reference is crystalline germanium at 77 K.

T, increases with increasing interatomic distance. So the thermal disorder in the first three shells of c-Ge shows significant differences; we will discuss this in the following. (c) The third cumulant is zero and temperature independent for the first shell; it is close to zero also for the outer shells indicating that the distance distributions present negligible asymmetry. (d) The fourth cumulant is zero and temperature independent only for the first shell. It increases with temperature for the second and third shells, indicating a symmetric deviation from Gaussian shape; an analogous result was found for the second and third shells of GaAs.[21] This confirms that, beyond the first shell, anharmonicity effects are not negligible even in systems with relatively high Debye temperature.

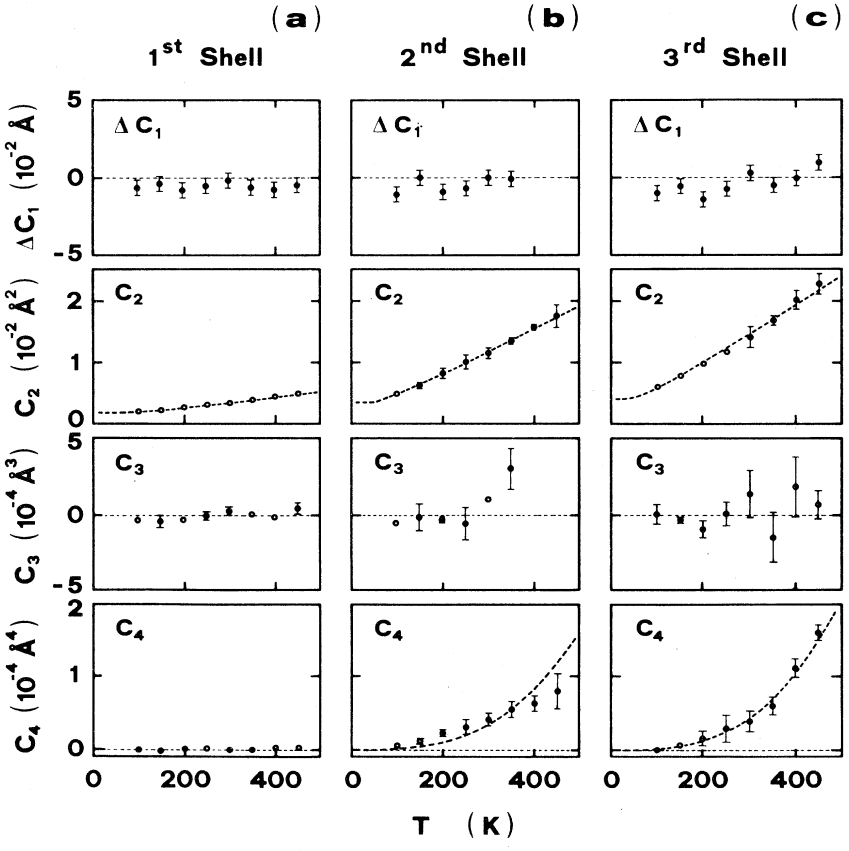

FIG. 5. Temperature dependence of the first four cumulants of the first three coordination shells of c-Ge (experimental dots). The $C_2(T)$ curves (dashed lines) represent the Einstein models best fitting the slope of the experimental data in the high temperature region to which experimental points have been normalized; the $C_4(T)$ curves (dashed lines) represent AT^3 functions best fitting the experimental data.

TABLE I. Einstein frequencies relative to the MSRD's of c-Ge and c-Ge (ω_E^{anhar} is related to the experimental MSRD, ω_E^{har} to the harmonic contribution to the MSRD). The temperature dependence of C_4 follows a AT^3 behavior.

	c-Ge			a-Ge
	First	Second	Third	
ω_E^{anhar} (THz)	7.50 ± 0.20	3.90 ± 0.11	3.48 ± 0.22	6.9 ± 0.2
ω_E^{har} (THz)	7.50 ± 0.45	4.27 ± 0.18	3.84 ± 0.18	
A (10^{12} Å^4 K^{-3})	0	1.32 ± 0.39	1.65 ± 0.46	

As for the reconstruction of the distance distributions from cumulants, we have found that within the examined temperature range the first shell distance distribution appears Gaussian, whereas the second and third shells show a non-Gaussian distance distribution with negligible asymmetry.

B. Amorphous germanium

In Fig. 6 the experimental cumulants of a-Ge, obtained by using 77 K c-Ge as reference compound, are reported: the difference between the first-nearest-neighbor distances of c-Ge and a-Ge and the overall disorder, thermal and static, of a-Ge are evident. ΔR represents the first shell distance differences $R_{a\text{-Ge}}(T) - R_{c\text{-Ge}}(77)$ (full circles) and $R_{c\text{-Ge}}(T) - R_{c\text{-Ge}}(77)$ (crosses): the interatomic distance of amorphous germanium is about 0.02 Å larger than that of crystalline germanium. The difference between $C_2(T)$ for c-Ge (lower curve) and a-Ge (upper curve) is mainly due to the static contribution to disorder. As for C_3 and C_4, they are significantly different from zero over the whole temperature range. These results show that the radial distribution of distances is not Gaussian even at low temperature; the temperature dependence of C_3 and C_4 shows a slight increase with increasing temperature suggesting a slight anharmonic character of thermal disorder.

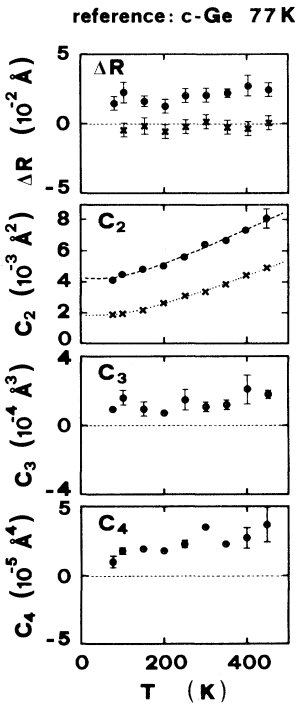

FIG. 6. Temperature dependence of the first four cumulants (circles) of the first coordination shell of a-Ge: analysis carried out using 77 K c-Ge as reference compound. [ΔR of crystalline germanium (crosses) reported for comparison.]

VI. DISCUSSION

A. Distribution of distances

In Fig. 7 the *real* distributions of distances of the first shell of c-Ge and a-Ge (Refs. 16 and 22) are reported for some temperatures. The characteristic function was reconstructed in the range -20–20 Å^{-1} with λ equal to 8 Å (no significant variations were observed on varying λ from 4 to 10 Å). The distributions of distances of the first shell of c-Ge, Fig. 7, do not show any evident asymmetry effect in the temperature range 77–400 K since the Debye temperature Θ_D of Ge is 374 K. This result is in agreement with the experimental result of Crozier and Seary,[4] who detected deviations from Gaussian only at temperatures (1085 K) higher than Θ_D. A manifest deviation from a Gaussian distribution due to thermal and

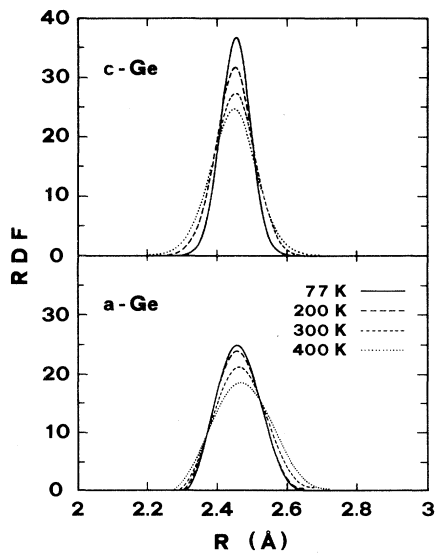

FIG. 7. The real distribution of distances of the first coordination shell of c-Ge and a-Ge at various temperatures.

static disorder is present in a-Ge (Fig. 7), even at low temperature. This result is in contrast with theoretical models which assume a regular tetrahedron as the basic unit of the amorphous Ge network.[23]

B. Thermal disorder in c-Ge

The widths of the distance distributions $C_2(T)$ in Figs. 5 and 6 represent the mean square relative displacement of backscattering atoms with respect to the absorbing atom. The MSRD is composed of two contributions: the mean square displacement of atoms from their equilibrium positions and the vibrational correlation function.[24] The latter contains integrated information on the projected density of vibrational states and thus on the phase relationships between phonon eigenvectors. For cubic metals the partial density of states has been successfully approximated by a Debye distribution taking into account the motion correlation.[24] This model has been found adequate to interpret the MSRD of the first three coordination shells of Cu, Pt, and Fe and is equivalent to more refined force constant models.[25] However, in polyatomic lattices, where optical phonons are present, as in zinc-blende or diamond lattices, the Debye approximation is no longer adequate to reliably reproduce the phonon spectrum. In certain cases phenomenological approaches based on hybrid Debye-Einstein approximations, with the Einstein model taking into account optic modes, have been applied.[26] When *ab initio* calculations or force constant models exist, one can determine and compare MSRD's directly with experiment. As for the MSRD of Ge, two theoretical calculations have been performed: the first one, by Nielsen and Weber,[27] is based on the adiabatic bond charge model and holds for some crystalline covalent semiconductors; the second one, by Filipponi,[28] is based on the high temperature expansion in moments of the projected density of states for the vibrational correlation function (VCF) and holds for some tetravalent crystalline and amorphous solids. Both calculations have been carried out in the harmonic approximation.

In order to compare the theoretical MSRD's with the experimental ones, we need to extract from the latter the harmonic contribution; the detailed procedure to do this is described in Ref. 22; here we give a brief summary. The pair potential is extracted by inverting the classical statistics relationship which relates the interatomic potentials to the distance distributions[29] reconstructed from the experimental cumulants (data in Figs. 5 and 6); the cumulants are then expanded as a power series of temperature whose terms depend on the force constants γ_n.[30] For harmonic potentials $\gamma_n = 0$ for $n > 2$ and C_2 depends linearly on temperature. For anharmonic potentials an additional term proportional to T^2 must be considered; at high temperature and for very anharmonic potentials higher order terms cannot be neglected. As for Ge, the series expansion of C_2 has been truncated at the second term. The results of this procedure are reported in Fig. 8 where the C_2 of the *effective* and *real* anharmonic distributions of the first three shells of c-Ge are shown

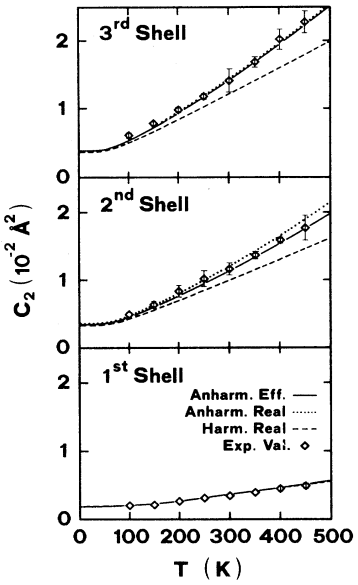

FIG. 8. Temperature dependence of second cumulants of the first three shells of c-Ge calculated from the force constants of pair potentials: continuous lines refer to *effective* anharmonic distributions, dotted lines to *real* anharmonic distributions; dashed lines represent the first order harmonic contribution of the *real* distributions. The experimental points (data from Fig. 5) are also reported.

(continuous and dotted lines, respectively) together with the first order harmonic contributions related to the real distributions (dashed lines) and the experimental points (data from Fig. 5). The good agreement between second order contributions to C_2 related to the *effective* distributions and experimental values constitutes an *a posteriori* test of the validity of the second order truncation. In Fig. 8 it is also worth observing the remarkable difference between the experimental values and the harmonic contribution to C_2 for the second and third coordination shells. This difference is significantly larger than the experimental uncertainty, including the estimated effects due to the interference between second and third shell peaks. The harmonic contributions to C_2 (dashed lines in Fig. 8) are reported in Fig. 9 at some temperatures (full circles, empty triangles, and squares for first, second, and third shells, respectively) to be compared with the theoretical MSRD calculated by Nielsen and Weber[27] [Fig. 9(a)] and by Filipponi[28] [Fig. 9(b)]. In Fig. 9(a) the lower curves represent bond charge model (BCM) calculations[27] of the correlated relative radial displacements for first and second neighbors in c-Ge (dashed and full lines, respectively); they are in good agreement with our first and second shell experimental data; not such a satisfactory agreement was found by the same authors[27] with the results of the correlated Debye model and the experimental data by Rabe *et al.*[31] The upper curve in Fig. 9(a) (dotted line) represents the theoretical uncorrelated Debye-Waller factor; its difference with respect to our third shell results (squares) expresses the residual correlation of motion between the central atom and

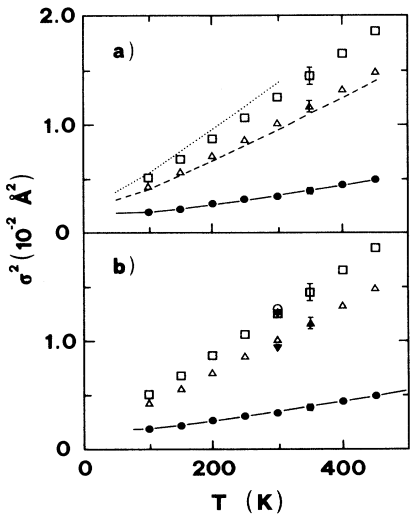

FIG. 9. Comparison between the harmonic contributions of the second cumulants of the first three coordination shells of c-Ge (present work: first shell, full circles; second shell, empty triangles; third shell, squares) and some theoretical MSRD's. (a) Comparison with theoretical data by Nielsen and Weber (Ref. 27) (first shell, full line; second shell, dashed line; mean square displacement, dotted line); (b) comparison with theoretical data by Filipponi (Ref. 28) (first shell, full line; second shell, at 300 K, full triangle; third shell, at 300 K, cross; mean square displacement, at 300 K, empty circle).

third shell backscattering atoms. The second theoretical method [Fig. 9(b)] determines the MSRD without solving the secular problem for the dynamical matrix[28] and calculates first shell MSRD's in a wide range of temperatures (full line) and second and third shell MSRD's at 300 K (full triangle and cross, respectively); these results are also in good agreement with our data.

C. Thermal and static disorder in a-Ge

The disorder parameters of a-Ge are represented in Fig. 6 and reported in Table II. The thermal dependence of C_2 in a-Ge is very close to that of the c-Ge first shell; for a-Ge the Einstein frequency is 6.9 ± 0.2 THz while for c-Ge it is 7.50 ± 0.20 THz. This means that the local thermal disorder in a-Ge is slightly smaller than in c-Ge as already observed by theoretical calculations.[28]

At room temperature the sum of the static and dynamic contributions to disorder [$C_2(300)$ in Fig. 6, here denoted σ^2] is $\sigma^2 = (6.4 \pm 0.1) \times 10^{-3}$ Å^{-2}, which is different from the value of 3.6×10^{-3} Å^{-2} reported by Shevchik and Paul[32] from x-ray diffraction measurements. The contribution of static disorder to the mean square relative displacement can be evaluated by extrapolating the σ^2 curves of c-Ge and a-Ge in Fig. 6 to very low temperature; the difference $\sigma^2_{\text{stat}} = \sigma^2_{a\text{-Ge}}(77) - \sigma^2_{c\text{-Ge}}(77) = (2.25 \pm 0.17) \times 10^{-3}$ Å^2 represents a measurement of static disorder of the evaporated thin film. This value is higher than the result of 0.9×10^{-3} Å^2 calculated by Polk[33] and close to the experimental value of 2.0×10^{-3} Å^2 reported by Wakagi *et al.*[34,35] from EXAFS measurements on samples prepared by sputtering.

Another interesting result of EXAFS amplitude analysis is the coordination number ratio $N_{a\text{-Ge}}(T)/N_{c\text{-Ge}}(77)$ obtained by leaving the ratio N_s/N_r as a free parameter. In the whole temperature range $N_{a\text{-Ge}}(T)/N_{c\text{-Ge}}(77) = 1.00 \pm 0.05$, which implies that the first shell average coordination number of a-Ge is 4.0 ± 0.2; as a test of accuracy for the determination of the coordination number by the ratio method, we found that for c-Ge $N_{c\text{-Ge}}(T)/N_{c\text{-Ge}}(77)$ was equal to 1 ± 0.03.

The amorphous germanium structure has been widely investigate by x-ray and neutron diffraction as well as by EXAFS (Table II). X-ray diffraction measurements carried out by Temkin *et al.*[36] found that the first shell distance and coordination number are equal respectively to $R = 2.47$ Å and $N = 3.79$; the corresponding

TABLE II. EXAFS and x-ray and neutron diffraction data about the local structure of a-Ge samples.

	N	R (Å)	C_2 (static) (10^{-3} Å^2)	C_2 (thermal) (THz)	C_3 (10^{-4} Å^3)	C_4 (10^{-5} Å^4)
c-Ge	4	2.4496		7.5		
a-Ge						
EXAFS						
Crozier and Seary (Ref. 4)	4	2.45	1.8	7.5		
Stern *et al.* (Ref. 6)	4	2.45				
Wakagi *et al.* (Refs. 34, 35)	3.90	2.469	2.0		1.2	
Present	4.0 ± 0.2	2.468 ± 0.005	2.25 ± 0.21	6.9 ± 0.2	1.07 ±0.42	3.52 ±0.15
Diffraction						
Temkin *et al.* (Ref. 36)	3.79	2.47				
Etherington *et al.* (Ref. 37)	3.69	2.463				
Wright *et al.* (Ref. 38)	3.67	2.465				

crystallographic data for c-Ge are $R = 2.4496$ Å and $N = 4$. Moreover, neutron diffraction measurements carried out by Etherington *et al.*[37] found $R = 2.463$ Å and $N = 3.68$; more recently, Wright *et al.*[38] reported the values $R = 2.465$ Å and $N = 3.67$. Thus, according to x-ray and neutron diffraction measurements, the a-Ge first shell distance is larger than the crystalline one and the first coordination number is smaller. Several important EXAFS works on a-Ge evaporated thin films are reported in the literature;[4–7] as far as structural investigation is concerned, they are generally based on the Gaussian approximation. The first shell distance and coordination number obtained by the previous standard EXAFS analysis are close to the crystalline data and in disagreement with diffraction results;[4,6] when higher order moments of the first-nearest-neighbor distribution have been taken into account, as in the case of a-Ge prepared by sputtering,[34,35] it is found that the first shell distance is longer than that of c-Ge by 0.019 Å. Therefore EXAFS cumulant analysis demonstrates that the first shell distance distribution is asymmetric, indicates the presence of a non-negligible static disorder even at low temperature, and finds that $R = 2.468$ Å in good agreement with the recent work by Wakagi *et al.*;[35] however, the coordination number obtained by all the EXAFS measurements (Table II) does not agree with the values less than 4 reported by x-ray and neutron diffraction data.[36,38]

VII. CONCLUSIONS

The cumulant analysis of EXAFS allows a refined study of parameters able to describe the local structure and dynamics in systems with low or moderate disorder. In this work we have reexamined the local order of germanium, in the crystalline and amorphous phases, by a temperature-dependent study of the amplitude and phase of EXAFS oscillations. In c-Ge the first three coordination shells, sufficiently well separated in real space and little influenced by multiple scattering contributions, have been Fourier transformed to k space and analyzed with the cumulant method by using experimental amplitude and phase shift functions. The first four cumulants allow the reconstruction of the radial distribution functions: a deviation from Gaussian behavior is found for the outer shells. Harmonic and anharmonic contributions to the MSRD in the first three shells have been separated on the basis of experimental data. In the temperature range 77–450 K the first shell EXAFS effective pair potential is harmonic; anharmonicity is present in the outer shells also below the Debye temperature. The agreement between the experimental harmonic MSRD's of the first three shells and the theoretical MSRD's based on the calculation of the vibrational correlation functions is a further demonstration of the capability of the EXAFS technique to give information about phonon eigenvectors. The complementarity of EXAFS to neutron scattering techniques to test refined models of vibrational dynamics is confirmed.

In amorphous germanium the distribution of nearest-neighbor atoms has been determined at various temperatures: it is asymmetric even at the lowest temperature because of the static disorder. The thermal and static contributions to local disorder have been separately evaluated. The relatively larger momentum transfer of EXAFS with respect to the x-ray diffraction technique makes EXAFS particularly sensitive to monitor and characterize anharmonicity.

ACKNOWLEDGMENTS

The authors would like to thank E. Burattini, S. Mobilio, A. Sadoc, and the respective technical staffs of PWA, PULS, and LURE facilities for their scientific and technical collaboration. The contributions of F. Boscherini, A. Kuzmin, and R. Gotter for helpful discussions are also acknowledged.

[1] E.D. Crozier, J.J. Rehr, and R. Ingalls, in *X-Ray Absorption: Principles, Applications, and Techniques of EXAFS, SEXAFS, and XANES*, edited by D.C. Koningsberger and R. Prins (J. Wiley & Sons, New York, 1989), p. 373.
[2] P.A. Lee, P.H. Citrin, P. Eisenberger, and B.M. Kincaid, Rev. Mod. Phys. **53**, 769 (1981).
[3] E.A. Stern, B.A. Bunker, and S.M. Heald, Phys. Rev. B **21**, 5521 (1980).
[4] E.D. Crozier and A.J. Seary, Can. J. Phys. **59**, 876 (1981).
[5] F. Evangelisti, M.G. Proietti, A. Balzarotti, F. Comin, L. Incoccia, and S. Mobilio, Solid State Commun. **37**, 413 (1981).
[6] E.A. Stern, C.E. Bouldin, B. von Roeden, and J. Azoulay, Phys. Rev. B **27**, 6557 (1983).
[7] M.A. Paesler, D.E. Sayers, R. Tsu, and J.G. Hernandez, Phys. Rev. B **28**, 4550 (1983).
[8] G.W. Johnson, D.E. Brodie, and E.D. Crozier, Can. J. Phys. **67**, 358 (1989).
[9] P. Eisenberger and G.S. Brown, Solid State Commun. **29**, 481 (1979).
[10] T.M. Hayes and J.B. Boyce, J. Phys. C **13**, L731 (1980).
[11] E.A. Stern, in *Physics of Disordered Materials*, edited by D. Adler, H. Fritzche, and S.R. Ovshinsky (Plenum Press, New York, 1985), p. 143.
[12] G. Bunker, Nucl. Instrum. Methods **207**, 437 (1983).
[13] J.M. Tranquada, and R. Ingalls, Phys. Rev. B **28**, 3520 (1983).
[14] E.A. Stern, Y. Ma, O. Hanke-Petitpierre, and C.E. Bouldin, Phys. Rev. B **46**, 687 (1992).
[15] L. Wenzel, D. Arvanitis, R. Rabus, T. Lederer, and K. Baberschke, Phys. Rev. Lett. **64**, 1765 (1990).
[16] G. Dalba, P. Fornasini, and F. Rocca, Phys. Rev. B **47**, 8502 (1993).
[17] E.A. Stern and K. Kim, Phys. Rev. B **23**, 3781 (1981).
[18] E.D. Crozier, J.J. Rehr, and R. Ingalls, in *X-Ray Absorption: Principles, Applications, and Techniques of EXAFS, SEXAFS, and XANES* (Ref. 1), p. 413.
[19] G. Dalba, P. Fornasini, D. Diop, A. Kuzmin, and F. Rocca, J. Phys. Condens. Matter **5**, 1643 (1993).
[20] J.J. Rehr, R.C. Albers, and S.I. Zabinsky, Phys. Rev. Lett.

69, 3397 (1992).
[21]G. Dalba, D. Diop, F. Fornasini, and F. Rocca, J. Phys. Condens. Matter **6**, 3599 (1994).
[22]G. Dalba, P. Fornasini, R. Gotter, and F. Rocca, Phys. Rev. B **52**, 149 (1995).
[23]F. Wooten, K. Winer, and D. Weaire, Phys. Rev. Lett. **54**, 1392 (1985).
[24]G. Beni and P.M. Platzman, Phys. Rev. B **14**, 1514 (1976).
[25]E. Sevillano, H. Meuth, and J.J. Rehr, Phys. Rev. B **20**, 4908 (1987).
[26]G. Dalba, P. Fornasini, F. Rocca, and S. Mobilio, Phys. Rev. B **41**, 9668 (1990).
[27]O.H. Nielsen and W. Weber, J. Phys. C **13**, 2449 (1980).
[28]A. Filipponi, Phys. Rev. B **37**, 7027 (1987).
[29]T. Yokoyama, T. Satsukawa, and T. Ohta, Jpn. J. Appl. Phys. **28**, 1905 (1989).
[30]J. Tranquada, Ph.D. thesis, University of Washington, Seattle, 1983.
[31]P. Rabe, G. Tolkiehn, and A. Werner, J. Phys. C **12**, L545 (1979).
[32]N.J. Shevchik and W. Paul, J. Non-Cryst. Solids **8-10**, 381 (1972).
[33]D.E. Polk, J. Non-Cryst. Solids **5**, 365 (1971).
[34]M. Wakagi, M. Chigasaki, and M. Nomura, J. Phys. Soc. Jpn. **56**, 1765 (1987).
[35]M. Wakagi and Y. Maeda, Phys. Rev. B **50**, 14 090 (1994).
[36]R.J. Temkin, W. Paul, and G.A.N. Connel, Adv. Phys. **22**, 581 (1973).
[37]G. Etherington, A.C. Wright, J.T. Wenzel, J.C. Dore, J.H. Clarke, and R.N. Sinclair, J. Non-Cryst. Solids **48**, 265 (1982).
[38]A.C. Wright, R.A. Hulme, D.I. Grimley, R.N. Sinclair, S.W. Martin, D.L. Price, and F.L. Galeener, J. Non-Cryst. Solids **129**, 213 (1991).